

# Crossover from Ising to mean-field critical behavior in an aqueous electrolyte solution

J. Jacob and A. Kumar

*Department of Physics, Indian Institute of Science, Bangalore 560 012, India*

M. A. Anisimov, A. A. Povodyrev, and J. V. Sengers

*Institute for Physical Science and Technology and Department of Chemical Engineering, University of Maryland, College Park, Maryland 20742*

(Received 23 February 1998)

The near-critical behavior of the susceptibility deduced from light-scattering measurements in a ternary liquid mixture of 3-methylpyridine, water, and sodium bromide has been determined. The measurements have been performed in the one-phase region near the lower consolute points of samples with different concentrations of sodium bromide. A crossover from Ising asymptotic behavior to mean-field behavior has been observed. As the concentration of sodium bromide increases, the crossover becomes more pronounced, and the crossover temperature shifts closer to the critical temperature. The data are well described by a model that contains two independent crossover parameters. The crossover of the susceptibility critical exponent  $\gamma$  from its Ising value  $\gamma=1.24$  to the mean-field value  $\gamma=1$  is sharp and nonmonotonic. We conclude that there exists an additional length scale in the system due to the presence of the electrolyte which competes with the correlation length of the concentration fluctuations. An analogy with crossover phenomena in polymer solutions and a possible connection with multicritical phenomena is discussed. [S1063-651X(98)06108-X]

PACS number(s): 05.70.Jk, 64.60.Fr, 64.60.Kw

## I. INTRODUCTION

A challenging problem of critical phenomena in complex fluids, such as polymer and micellar solutions, microemulsions, and solutions of electrolytes, is to account for an interplay between universality caused by long-range fluctuations of the order parameter and a specific supramolecular structure. The approach to universal critical behavior in such systems should be affected by a competition between the correlation length of the critical fluctuations and an additional length associated with the supramolecular structure or/and with long-range interparticle interactions. Hence, even within the asymptotic Ising-like universality class, complex fluids may exhibit different crossover behavior upon approaching the critical point. Experimental studies of near-critical micellar and ionic solutions have yielded contradictory results [1–10]. Degiorgio and co-workers [1,2] reported nonuniversal (system-dependent) near-critical behavior in micellar solutions. Light-scattering studies of Dietler and Cannell [3] and Hamano *et al.* [4] showed that micellar solutions do exhibit asymptotic Ising-like universal behavior. However, the character of the approach to the universal asymptotic regime remains unknown, and the physical reasons for the observed discrepancies between results reported in Refs. [1,2] and [3,4] are still unexplained. Experimental results for ionic fluids, which suggest either mean-field (classical) behavior [5,9] or Ising-like nonclassical behavior [6–8,10], have been reported.

The discussion of the nature of criticality in ionic systems (see Refs. [11–15]) has recently received a new impetus after experimental data obtained by Narayanan and Pitzer for several low-dielectric-constant ionic solutions showed unusual sharp crossover from Ising asymptotic behavior to mean-field behavior [16–18]. It has been observed that mean-field behavior is more pronounced in systems with

low-dielectric-constant solvents. Narayanan and Pitzer explained this phenomenon by the presence of unscreened long-range Coulombic interactions in such systems. Ising critical behavior has been observed in certain apparently ionic systems where the phase separation is believed to be driven by short-range hydrogen-bonded interactions [6–8]. Moreover, sometimes, just as earlier for micellar solutions [2,3], different studies indicate either mean-field [9] or Ising behavior [10] even for the same ionic system, if the samples have a different origin.

Anisimov *et al.* [19] showed that the sharp crossover behavior in ionic solutions can be quantitatively described by a crossover model that contains two independent crossover parameters associated with two different characteristic spatial scales. In low-dielectric-constant ionic systems, for example, these scales may reflect two different ranges of interparticle interactions: short-range solvophobic and long-range Coulombic. Elucidation of the critical behavior in other complex fluids may need a similar approach. A qualitatively sharp crossover to mean-field behavior and mesoscopic-range structure has been reported earlier for metal-ammonia solutions [20]. Crossover between Ising-like asymptotic behavior and mean-field classical behavior has also been reported for polymer blends [21–23] and for a microemulsion system [24]. Attempts [21,23,24] have been made to describe these data in terms of a version of the crossover theory that contains a single crossover scale [25,26]. On the other hand, solutions of polymers in low-molecular-weight solvents exhibit sharp nonmonotonic crossover behavior when the correlation length of the critical fluctuations and the polymer molecular size, as specified by the radius of gyration, are of the same order [27]. The description of this crossover phenomenon requires two independent parameters associated, respectively, with intramolecular and intermolecular correlations. Moreover, the crossover behavior in polymer solutions

is affected by the presence of a tricritical  $\theta$  point [28]. Since tricritical behavior is mean-field-like in three dimensions, the observed phenomenon is, in fact, a crossover from the asymptotic Ising regime to the mean-field tricritical regime. The question arises: do critical crossover phenomena have a universal character for complex fluids? Will the additional length scale always be associated with an additional order parameter and, hence, with multicritical phenomena like in polymer solutions? Further progress in understanding the nature of critical phenomena in complex fluids depends on more comprehensive and more accurate experimental studies. It must be noted that nonaqueous ionic fluids and surfactant solutions are very sensitive to impurities and may be chemically unstable, so that results of measurements may not be reproducible [1–3,9,10]. In this work we report a study of the near-critical behavior of the susceptibility deduced from light-scattering measurements in a ternary liquid mixture which is free from the disadvantages mentioned before.

Multicomponent liquid mixtures have been a subject of study during the past few years [29–32]. In some cases ternary liquid mixtures with an electrolyte as a component were treated as quasibinary systems, since the amount of electrolyte added was quite small and the overall concentration of the electrolyte could be treated as a hidden field variable [30]. Although it has been well established that these systems belong to the Ising universality class [30–32], a trend toward mean-field behavior has also been observed [31,32]. An electrolyte-induced structuring was tentatively proposed [31,32] as a possible reason for this trend. As the amount of electrolyte is increased, there could be a competition between a length scale due to this structuring and the correlation length of the concentration fluctuations. Such a competition could lead to mean-field critical behavior in a region away from the relevant consolute critical point, where this additional length scale overrides the correlation length.

To clarify these issues we have examined the crossover behavior of the susceptibility of the system 3-methylpyridine (MP)+water ( $H_2O$ )+sodium bromide (NaBr). NaBr was selected as the electrolyte after exhaustive trials with several other salts. The system MP+ $H_2O$  is completely miscible at all temperatures at atmospheric pressure. An immiscibility gap with loop size  $\Delta T=(T_U-T_L)$ ,  $T_U$  being the upper critical solution temperature and  $T_L$  the lower critical solution temperature, appears in this system starting from a “double” critical point (where  $T_U=T_L$ ) with the addition of an electrolyte like NaCl ( $\sim 0.1$  wt %) or NaBr ( $\sim 0.4$  wt %) [30]. If an experimental path is tangential to the critical line at the double critical point, a doubling of the critical exponents is observed [30,33]. With the addition of such electrolytes, the polar hydroxyl groups in MP and  $H_2O$  become increasingly shielded from one another, reducing the strength of the hydrogen-bond and dipolar forces and thus lowering  $T_L$ . Since the radius of the chlorine ion (1.81 Å) is smaller than that of the bromide ion (1.96 Å), NaCl causes a more drastic shift in  $T_L$  than the same amount of NaBr does. With further increase in the electrolyte concentration,  $\Delta T$  increases, i.e.,  $T_L$  decreases and  $T_U$  increases as shown in Fig. 1, where we have plotted the critical solution temperature as a function of the mass fraction of NaBr.

We have observed a crossover of the susceptibility from asymptotic Ising-like behavior to mean-field behavior. The

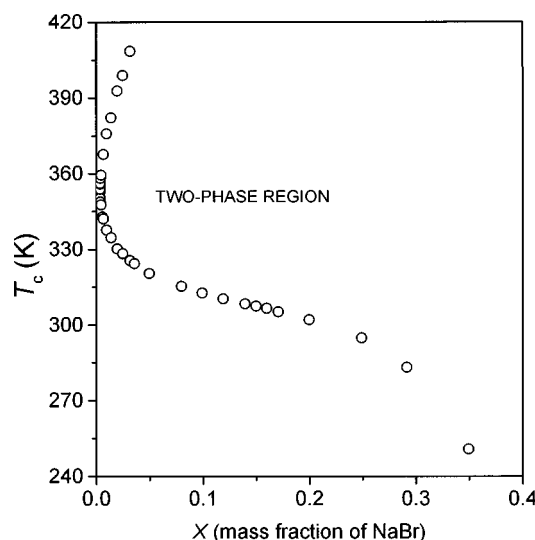


FIG. 1. Upper and lower critical solution temperatures (the upper branch is  $T_c=T_U$  and the lower branch is  $T_c=T_L$ ) as a function of the mass fraction of NaBr for the 3-methylpyridine+water+sodium bromide system.

crossover becomes more and more pronounced as the concentration of NaBr increases. The data are well described by a crossover model developed by Chen and co-workers [34,35], and applied previously to elucidate the crossover behavior of the susceptibility of some ionic and polymer solutions [19,27], which contains two independent crossover parameters. The crossover of the susceptibility critical exponent  $\gamma$  from its Ising value  $\gamma=1.24$  to the mean-field value  $\gamma=1$  is sharp and nonmonotonic. We conclude that there exists an additional length scale in the system due to the presence of the electrolyte which competes with the correlation length of the concentration fluctuations. A striking analogy with the crossover behavior observed for semidilute polymer solutions and the possibility of multicritical phenomena at higher concentrations of sodium bromide are discussed.

## II. EXPERIMENT

We prepared the samples using MP (from Aldrich with a stated purity of 99%), water (triple distilled in an all-quartz distiller) and freshly dried analytical grade NaBr. The samples (about  $5\text{ cm}^3$ ) were initially prepared in cylindrical pyrex glass cells. The lower critical temperatures were measured in a well stirred liquid paraffin thermostat with a temperature stability better than  $\pm 1$  mK. A visual observation of the onset of opalescence and of the eventual formation of a meniscus after a typical temperature quench of 3 mK has been used to determine  $T_L$ . The critical concentration of MP,  $x_{MP}=(x_{MP})_c$ , ( $x_{MP}$  being the mass fraction of MP in the ternary mixture) for each value of  $X$  (overall mass fraction of NaBr) was accurately determined by preparing six or seven samples close to  $(x_{MP})_c$  for each  $X$  and then measuring their phase-separation temperatures. For the critical sample, the meniscus forms exactly at the center of the cell. It should be noted that the critical concentration  $(x_{MP})_c$  of MP may not coincide with the concentration  $(x_{MP})_e$  corresponding to the extremum of the phase-separation boundary because of

TABLE I. Properties of the 3-methylpyridine(MP)+water(H<sub>2</sub>O)+sodium bromide(NaBr) samples. Note that  $X$  and  $\tilde{X}$  denote the mass and the mole fraction of NaBr in the mixture, respectively;  $(x_{\text{MP}})_c$  is the critical mass fraction of MP in the mixture;  $\rho$  is the density at 25 °C.

Sample	$X$	$(x_{\text{MP}})_c$	$\tilde{X}$	$T_L(=T_c)$ (K)	$\rho(\text{g cm}^{-3})$	$\frac{1}{T_c} \frac{dT_c}{d\tilde{X}}$
1	0.0800	0.2791	0.019 75	315.115 ± 0.005	1.0570	-1.68
2	0.1190	0.2616	0.030 16	310.237 ± 0.002	1.0905	-1.30
3	0.1396	0.2523	0.035 88	308.140 ± 0.004	1.1083	-1.08
4	0.1500	0.2467	0.038 77	307.326 ± 0.004	1.1177	-0.962
5	0.1600	0.2403	0.041 55	306.435 ± 0.004	1.1270	-0.852

the obliqueness of the coexistence surface for a ternary liquid mixture [30]. For example, at  $X=0.1500$ ,  $(x_{\text{MP}})_c=0.2467 \pm 0.0001$  and  $(x_{\text{MP}})_e=0.4250 \pm 0.0001$ ; at  $X=0.0800$ ,  $(x_{\text{MP}})_c=0.2791 \pm 0.0001$  and  $(x_{\text{MP}})_e=0.4232 \pm 0.0001$ . Table I shows that there is a gradual variation of  $(x_{\text{MP}})_c$  as  $X$  varies from 0.08 to 0.16. For the samples used in the light-scattering runs the upper critical temperatures were not determined, since they were invariably above 150 °C.

The samples used for the light-scattering measurements were first prepared in pyrex glass cells and then transferred to the light-scattering cells (volume  $\approx 0.3 \text{ cm}^3$ ) by means of air-tight (Hamilton) syringes fitted with millipore filters (pore size 0.2  $\mu\text{m}$ ). These cells were flame sealed after the samples had been frozen in liquid nitrogen. The samples were well stirred for about 15–20 min in an ultrasonic agitator after preparation, and also before starting each light-scattering run. We checked  $T_L$  and the criticality of the samples both before and after measuring the scattered-light intensity as a function of temperature for each sample by monitoring the vanishing of the transmitted laser beam and the appearance of a meniscus at the center of the cell. We did not detect any drift in the value of  $T_L$  over the duration of the measurements for a given sample.

The sample cell was placed in a brass-block thermostat that has a temperature stability better than  $\pm 1$  mK in the temperature range 25–90 °C [36]. The temperature  $T$  of the sample was measured with a ruggedized thermistor [37] placed very close to the sample cell. The thermistor was calibrated in terms of IPTS-68. The laser beam (632.8 nm) from a He-Ne laser (5 mW) was focused at the center of the sample cell. To reduce the contribution from multiple scattering, we designed the cell so that the optical path length was less than 8 mm. The height of the sample was less than 7 mm. The transmitted and incident beam intensities were measured with photodiodes. The scattered-light intensity (at 90°) was detected with a photomultiplier tube whose output was fed to a photon counter through a fast preamplifier (EG & G ORTEC). The light-scattering apparatus was the same one as used earlier for experiments near double [30] and quadruple [31] critical points, but with some refinements in terms of its optics, collection geometry, and electronics.

A typical run lasted about 25–30 h and covered the temperature range  $0.15 \text{ K} \leq (T_L - T) \leq 7 \text{ K}$  except for the sample with  $X=0.16$ , where the range was  $0.1 \text{ K} \leq (T_L - T) \leq 5 \text{ K}$ . The typical equilibration time was  $\sim 20$ –25 min for a temperature step of 0.1 K, and this time was roughly the same for all the samples. Thermal equilibrium was indi-

cated by the invariance of the scattered and transmitted intensities with time. Data very close to  $T_L$  ( $T_L - T < 0.1 \text{ K}$ ) were not taken into consideration so as to avoid complications due to multiple scattering and gravity effects. We performed both heating and cooling runs, and found that the results were completely reproducible. The light-scattering data were collected as the lower critical temperature  $T_L$  of the sample was approached by heating from the one-phase region. The measured scattered-intensity data have been corrected for extinction due to increased turbidity near the critical point as discussed by Bray and Chang [38]. Fluctuations in the incident light intensity were accounted for by normalizing the data with respect to the corresponding incident light intensity. The normalized intensity data  $I_s$ , corrected for extinction, are presented in Table II together with the associated uncertainty  $\delta I_s$ . Here  $\delta I_s$  is an absolute cumulative uncertainty calculated by propagation of errors due to the uncertainties in the counting statistics, the reference intensity, and the temperature. We did not observe any background intensity above the random error, and no detectable light scattering exceeding the noise was present at temperatures 10% away from the critical temperature.

### III. THEORY

In fluids with short-range intermolecular interactions the critical fluctuations affect the behavior of physical properties in a wide region around the critical point; in fact, wherever the correlation length exceeds the molecular size [39]. A property of one-component fluids such as the isothermal compressibility exhibits a tendency to cross over from universal asymptotic Ising-like behavior toward mean-field (van der Waals-like) behavior when the distance from the critical point increases and the correlation length decreases [25,39]. This crossover behavior is characterized by a single crossover scale, the Ginzburg number  $N_G$ , that is to be compared with the distance to the critical point  $\tau = |T - T_c|/T$ . In our case the critical temperature  $T_c$  is to be identified with  $T_L$ . For simple fluids the Ginzburg number is of the order  $\approx 0.01$ , so that the critical fluctuations can be neglected at  $\tau \gg 10^{-2}$  [25]. This is why, in practice, the crossover in simple fluids is never completed within the critical domain. In ordinary binary liquid mixtures the Ginzburg number is often even larger and the crossover is hardly observable [19].

The intensity of light scattered by the critical fluctuations is proportional to the susceptibility  $\chi$ , which in turn is proportional to the isothermal compressibility in one-component

TABLE II. The corrected light-scattering intensity data in arbitrary units as a function of  $T_L - T$ .

$T_L - T$ (K)	$I_s$ (arb. units)	$\delta I_s$ (arb. units)	$T_L - T$ (K)	$I_s$ (arb. units)	$\delta I_s$ (arb. units)
X=0.0800					
7.466	72.27	2.74	1.990	401.27	4.88
6.668	87.41	2.81	1.794	447.05	5.17
6.051	96.58	3.00	1.596	530.98	5.46
5.547	108.29	3.03	1.447	594.37	5.74
5.033	125.30	3.16	1.245	729.06	6.28
4.552	136.62	3.26	1.094	855.49	6.78
4.106	156.75	3.45	0.941	1049.56	7.41
3.697	188.84	3.61	0.839	1200.31	7.95
3.376	206.65	3.80	0.737	1431.55	8.68
3.144	227.58	3.90	0.582	1900.35	9.97
2.909	245.02	4.00	0.426	2837.93	12.34
2.672	279.86	4.22	0.270	4934.44	17.00
2.427	309.97	4.41	0.164	8760.92	24.63
2.234	342.54	4.60			
X=0.1190					
7.153	61.95	2.39	2.396	240.64	3.72
6.662	68.85	2.46	1.999	298.90	4.01
6.261	70.71	2.52	1.594	400.10	4.54
5.854	76.04	2.56	1.183	584.76	5.35
5.507	80.14	2.56	1.101	655.53	5.60
5.158	87.86	2.65	1.044	700.98	5.72
4.838	101.06	2.72	0.916	819.18	6.19
4.514	107.92	2.78	0.790	999.92	6.78
4.187	119.82	2.91	0.663	1232.89	7.52
3.855	126.84	2.94	0.533	1660.92	8.67
3.516	147.72	3.13	0.406	2315.97	10.32
3.174	167.29	3.22	0.276	3739.23	13.42
2.787	193.29	3.38	0.125	9416.40	22.95
X=0.1396					
6.875	57.27	2.08	1.893	258.63	3.43
6.262	61.43	2.11	1.594	322.80	3.74
5.793	69.87	2.18	1.390	388.38	4.23
5.476	70.49	2.24	1.063	541.20	4.67
5.089	79.07	2.27	0.793	767.46	5.44
4.729	82.44	2.31	0.558	1203.04	6.80
4.363	87.85	2.37	0.480	1469.23	7.51
3.993	100.34	2.46	0.401	1822.53	8.40
3.649	117.78	2.59	0.362	2122.54	9.08
3.302	130.78	2.68	0.256	3231.58	11.36
2.949	144.94	2.78	0.215	3919.01	12.69
2.592	173.62	2.99	0.135	6479.48	17.19
2.226	216.65	3.21			
X=0.1500					
6.206	41.49	2.44	1.592	201.66	4.31
5.750	43.12	2.47	1.226	278.55	4.99
5.288	48.11	2.57	0.967	374.12	5.70
4.816	48.98	2.60	0.780	497.91	6.50
4.335	61.08	2.76	0.629	645.49	7.30
3.845	66.58	2.85	0.516	836.20	8.31
3.444	75.45	2.98	0.439	1006.54	9.15
3.003	94.31	3.23	0.363	1288.64	10.34
2.657	107.15	3.38	0.286	1686.75	11.91
2.307	125.97	3.60	0.209	2403.23	14.53
1.952	157.75	3.94	0.133	3883.21	19.38
X=0.1600					
5.171	37.39	1.99	0.995	152.54	2.99
4.557	41.03	2.02	0.815	192.33	3.21
3.931	43.32	2.03	0.670	238.65	3.55
3.288	46.96	2.06	0.525	318.67	3.95
2.627	57.27	2.22	0.415	427.51	4.47
2.221	63.49	2.28	0.341	530.31	4.96
1.876	74.71	2.38	0.267	693.41	5.60
1.601	89.16	2.47	0.192	966.99	6.61
1.351	107.33	2.65	0.119	1598.20	8.70
1.174	129.58	2.81	0.063	2668.69	12.01

fluids and with the osmotic susceptibility in “incompressible” binary liquid mixtures or with a combination of osmotic susceptibilities in multicomponent liquid mixtures [40,41]. In zero ordering field (along the critical isochore in one-component fluids or along the critical concentration in binary mixtures, respectively) in the one-phase region asymptotically close to the critical point the susceptibility behaves as

$$\chi = \Gamma_0 \tau^{-\gamma} (1 + \Gamma_1 \tau^{\Delta_s} + \Gamma_2 \tau^{2\Delta_s} + a_1 \tau + \dots), \quad (1)$$

where  $\gamma = 1.239 \pm 0.002$  [42,43] and  $\Delta_s = 0.54 \pm 0.03$  [44] are universal critical exponents (actually we adopted  $\Delta_s = 0.51$ ), and where  $\Gamma_0$ ,  $\Gamma_1$ ,  $\Gamma_2$ , and  $a_1$  are system-dependent amplitudes. Expansion (1) is called the Wegner series [45]. Since real fluids do not obey the symmetry of the lattice gas, the susceptibility  $\chi$  also contains terms proportional to  $\tau^{-\alpha}$  [33,46] and  $\tau^{-\gamma+\Delta_a}$  [47–49] which are, however, weaker than the second Wegner correction term  $\sim \tau^{-\gamma+2\Delta_s}$ , as  $\alpha \approx 0.11$  and  $\Delta_a \approx 1.32$ .

In a wider region around the critical point, the susceptibility of fluids may exhibit a trend from universal Ising-like behavior to mean-field (van der Waals-like) behavior [25,26,50–55]. If one defines an effective susceptibility exponent as  $\gamma_{\text{eff}} = -\tau d \ln \chi / d\tau$  [50–52], a positive value of  $\Gamma_1$  means that  $\gamma_{\text{eff}}$  approaches the asymptotic value  $\gamma \approx 1.24$  from below, providing a smooth crossover from the mean-field value  $\gamma = 1$  far away from the critical point. Such a smooth crossover to the mean-field regime, although never completed in the critical domain, is exhibited by simple fluids [19]. In this case the crossover is basically controlled by the Ginzburg number, a single crossover parameter, that is responsible both for the convergence of the Wegner series (1) and for the range of validity of the mean-field approximation [25]. Recently, universal single-parameter crossover has been demonstrated by computer simulations of the two-dimensional Ising model [56]. However, there are several indications that such a simple monotonic crossover with positive  $\Gamma_1$  in the one-phase region is not universal. Liu and Fisher [57] concluded that for the nearest neighbor simple cubic, bcc, and fcc three-dimensional Ising lattices, the first correction amplitudes for the susceptibility, correlation length, specific heat capacity, and order parameter are negative, so that  $\gamma_{\text{eff}}$  asymptotically approaches  $\gamma \approx 1.24$  from above. The possibility of negative Wegner corrections follows from field-theoretical renormalization-group approaches [58,59]. Moreover, negative correction amplitudes have been reported for some aqueous solutions near the consolute critical point [60,61], whereas for other fluid systems [62,63] the correction amplitudes are positive. Narayanan and Pitzer have performed an extensive study of the near-critical turbidity of several nonaqueous ionic solutions [16–18]. They fitted the susceptibility and the correlation length, extracted from the turbidity data, to the Wegner expansion (1), and found that the character of the nonasymptotic behavior is strongly affected by the dielectric constant of the solvent. In particular, in their latest paper [18] they indicated a possible negative  $\Gamma_1$  for at least two of the systems investigated. Most recently, a crossover of the susceptibility with negative  $\Gamma_1$  has been observed near the consolute point of polystyrene in deuterocyclohexane by small-angle neutron

scattering [27]. With negative  $\Gamma_1$  the crossover of  $\gamma_{\text{eff}}$  from  $\gamma \approx 1.24$  to  $\gamma = 1$  will be nonmonotonic and sharper than usual.

It has been shown that the crossover behavior of the susceptibility observed in nonaqueous ionic solutions [19] and in polymer solutions in a low-molecular-weight solvent [27] can be adequately described by a crossover model which includes two independent crossover parameters. This model is based on renormalization-group (RG) matching [34,64,65] for the free-energy density. The critical part of the dimensionless free-energy density  $\Delta \tilde{A}$  is a function of a rescaled temperature distance  $t = c_t \tau$  to the critical point and of a rescaled order parameter  $M = c_p \varphi$ , where  $c_t$  and  $c_p$  are system-dependent amplitudes related to the range of intermolecular interaction, and where  $\varphi$  is the order parameter. At the vapor-liquid critical point of a one-component fluid the order parameter is associated with density, and at the liquid-liquid critical point of a mixture with concentration. As a result of the long-range fluctuations of the order parameter, the critical part  $\Delta \tilde{A}$  of the dimensionless free-energy density  $\tilde{A}$  is renormalized upon approaching the critical point in such a way that [34]

$$\Delta \tilde{A} = \frac{1}{2} t M^2 Y^{(\gamma-1)/\Delta_s} + \frac{1}{4!} u^* \bar{u} \Lambda M^4 Y^{(2\gamma-3\nu)/\Delta_s} - \frac{1}{2} t^2 \frac{\nu}{\alpha \bar{u} \Lambda} (Y^{-\alpha/\Delta_s} - 1), \quad (2)$$

where  $\nu = (2 - \alpha)/3 = 0.630 \pm 0.001$  is the critical exponent of the asymptotic power law for the correlation length [42,43]. The crossover function  $Y$  is to be determined from [35]

$$1 - [1 - \bar{u}] Y = \bar{u} \left[ 1 + \left( \frac{\Lambda}{\kappa} \right)^2 \right]^{1/2} Y^{\nu/\Delta_s}. \quad (3)$$

The last term in Eq. (2) is a so-called kernel term responsible for the weak singularity of the weak susceptibility (isochoric heat capacity in one-component fluids). The parameter  $\kappa$  is inversely proportional to the correlation length  $\xi$ . In zero field in the one-phase region the expression for  $\kappa^2$  reads [34]

$$\kappa^2 = c_t \tau Y^{(2\nu-1)/\Delta_s}. \quad (4)$$

In Eqs. (2) and (4) the normalized coupling constant  $\bar{u}$  and the “cutoff”  $\Lambda$  ( $\Lambda^{-1} = \xi_D v_0^{-1/3}$ , with  $\xi_D$  a characteristic length reflecting the discrete structure of the fluid and  $v_0$  the average molecular volume) are crossover parameters, while  $u^*$  is a universal RG fixed-point coupling constant. For three-dimensional Ising-like systems,  $u^* = 0.472$  [66]. Far away from the critical point in the mean-field region, Eq. (2) transforms into the critical part of the mean-field (“classical”) free-energy density:

$$\Delta \tilde{A} = \frac{1}{2} t M^2 + \frac{1}{4!} u^* \bar{u} \Lambda M^4. \quad (5)$$

TABLE III. The limiting behavior of the crossover function  $Y$ , the susceptibility  $\chi$ , the correlation length  $\xi$  in zero field in the one-phase region, and the order parameter  $\varphi$  along the phase boundary of the two-phase region.

Mean-field limit ( $\Lambda/\kappa \ll 1$ )	Critical point limit ( $\Lambda/\kappa \gg 1$ )
crossover function $Y$	
$Y = 1 - \frac{\bar{u}\Lambda^2/2}{c_t\tau[1 + \bar{u}(\nu/\Delta_s - 1)]}$	$Y = \left(\frac{\sqrt{c_t}}{\bar{u}\Lambda}\right)^{2\Delta_s} \tau_{\Delta_s} \left[ 1 - 2\Delta_s(1 - \bar{u}) \left(\frac{\sqrt{c_t}}{\bar{u}\Lambda}\right)^{2\Delta_s} \tau_{\Delta_s} \right]$
susceptibility $\chi$	
$\chi = a_0^{-1}(\tau - \tau_s)^{-1}$ $a_0 = c_t c_\rho^2$	$\chi = \Gamma_0 \tau^{-\gamma}(1 + \Gamma_1 \tau^{\Delta_s} + \dots)$ $\Gamma_0 = \left(\frac{\bar{u}\Lambda}{\sqrt{c_t}}\right)^{2(\gamma-1)} \frac{(1 + u^* \nu/2)^{-1}}{a_0}$
$\tau_s \approx \frac{\bar{u}\Lambda^2(\gamma - 1 - u^* \nu/2)}{2c_t \Delta_s [1 + \bar{u}(\nu/\Delta_s - 1)]}$	$\Gamma_1 = 2 \left( \gamma - 1 + \frac{u^* \nu \Delta_s}{2 + u^* \nu} \right) (1 - \bar{u}) \left(\frac{\sqrt{c_t}}{\bar{u}\Lambda}\right)^{2\Delta_s}$
correlation length $\xi$	
$\xi = \bar{\xi}_0(\tau - \tau_s)^{-1/2}$ $\bar{\xi}_0 = \left(\frac{c_0}{a_0}\right)^{1/2} = v_0^{1/3} c_t^{-1/2}$	$\xi = \xi_0 \tau^{-\nu}(1 + \xi_1 \tau^{\Delta_s})$ $\xi_0 = \bar{\xi}_0 \left(\frac{\bar{u}\Lambda}{\sqrt{c_t}}\right)^{2\nu-1}$ $\xi_1 = (2\nu - 1)(1 - \bar{u}) \left(\frac{\sqrt{c_t}}{\bar{u}\Lambda}\right)^{2\Delta_s}$
order parameter $\varphi$	
$\varphi = \pm \bar{B}_0  \tau - \tau_s ^{1/2}$ $\bar{B}_0 = \left(\frac{6a_0}{u_0}\right)^{1/2} = c_\rho^{-1} \left(\frac{6c_t}{u^* \bar{u}\Lambda}\right)^{1/2}$ $\tau_s \approx \frac{\bar{u}\Lambda^2(1 - 2\beta)}{2c_t \Delta_s [1 + \bar{u}(\nu/\Delta_s - 1)]}$	$\varphi = \pm B_0  \tau ^\beta (1 + B_1  \tau ^{\Delta_s} + \dots)$ $B_0 = b_0 \left(\frac{c_t^{1/2}}{\bar{u}\Lambda}\right)^{2\beta} \frac{(\bar{u}\Lambda)^{1/2}}{c_\rho}$ $B_1 = b_1 \left(\frac{c_t^{1/2}}{\bar{u}\Lambda}\right)^{2\Delta_s} (1 - \bar{u})$ $(b_0 \approx 2.98, b_1 \approx 0.531)$

The crossover parameters  $\bar{u}$  and  $\Lambda$  and the amplitudes  $c_t$  and  $c_\rho$  are related to the coefficients of the local (coordinate dependent) density of the classical Landau-Ginzburg free energy  $A$  [67]:

$$\begin{aligned} \frac{v_0}{k_B T} \frac{d(\Delta A)}{dV} &= \frac{1}{2} a_0 \tau \varphi^2 + \frac{1}{4!} u_0 \varphi^4 + \frac{1}{2} c_0 (\nabla \varphi)^2 \\ &= \frac{1}{2} t M^2 + \frac{1}{4!} u^* \bar{u} \Lambda M^4 + \frac{1}{2} (\bar{\nabla} M)^2, \end{aligned} \quad (6)$$

with  $a_0 = c_\rho^2 c_t$ ,  $u_0 = u^* \bar{u} \Lambda c_\rho^4$ ,  $c_0 = c_\rho^2 v_0^{2/3}$ , and  $\bar{\nabla} = v_0^{1/3} \nabla$ . The prefactor  $v_0/k_B T$ , where  $k_B$  is Boltzmann's constant, makes the free-energy density dimensionless.

The crossover equations for the dimensionless inverse susceptibility  $\chi^{-1}$  and correlation length  $\xi$  in zero field in the one-phase region ( $M=0$ ), implied by Eqs. (2) and (3), are [19]

$$\chi^{-1} = c_\rho^2 c_t \tau Y^{(\gamma-1)/\Delta_s} (1 + y), \quad (7)$$

$$\xi = v_0^{1/3} \kappa^{-1} = v_0^{1/3} [c_t \tau Y^{(2\nu-1)/\Delta_s}]^{-1/2}, \quad (8)$$

with

$$\begin{aligned} y &= \frac{u^* \nu}{2\Delta_s} \left\{ 2 \left(\frac{\kappa}{\Lambda}\right)^2 \left[ 1 + \left(\frac{\Lambda}{\kappa}\right)^2 \right] \left[ \frac{\nu}{\Delta_s} + \frac{(1 - \bar{u})Y}{1 - (1 - \bar{u})Y} \right] \right. \\ &\quad \left. - \frac{2\nu - 1}{\Delta_s} \right\}^{-1}. \end{aligned} \quad (9)$$

The expressions for the properties in the two-phase region are found from the equilibrium condition [68]

$$(\partial \Delta \tilde{A} / \partial M)_t = 0. \quad (10)$$

Upon increasing the distance from the critical point, this crossover model provides a continuous transformation from Ising-like, asymptotically close to the critical point, to mean-field behavior far away from the critical point. The transformation is controlled by the ratio  $\Lambda/\kappa$  or, equivalently, by the ratio of the correlation length over the microscopic characteristic length  $\xi/\xi_D$ . As shown in Table III, the equations for the crossover susceptibility and the correlation length in the one-phase region, and also for the order parameter in the two-phase region, exhibit Ising-like critical behavior asymptotically close to the critical point, whereas the classical (mean-field) expressions are recovered far away from the

critical point. Due to the critical fluctuations, the position of the actual critical temperature  $T_c$  is shifted with respect to the mean-field critical temperature  $\bar{T}_c$ . The critical temperature shift  $\tau_s = (\bar{T}_c - T_c)/T_c$  can be evaluated from different properties such as the inverse susceptibility or the order parameter. These different evaluations of  $\tau_s$  are proportional to a unique combination of the two crossover parameters ( $\bar{u}\Lambda^2 c_t$ ), whereas the critical amplitudes are functions of the product  $\bar{u}\Lambda$  (Table III).

For very large values of  $\Lambda$ , i.e., when cutoff effects are negligibly small, Eq. (3) for the crossover function  $Y$  can be approximated by

$$1 - [1 - \bar{u}]Y = \left( \frac{\bar{u}\Lambda}{\kappa} \right) Y^{\nu/\Delta_s}. \quad (11)$$

In this approximation the two crossover parameters  $\bar{u}$  and  $\Lambda$  in the crossover equations collapse into a single one,  $\bar{u}\Lambda$ , which is related to the Ginzburg number  $N_G$  [25]

$$N_G = g_0 \frac{(\bar{u}\Lambda)^2}{c_t} = g_0 \frac{u_0^2 v_0^2}{a_0^4 \bar{\xi}_0^6}, \quad (12)$$

with  $g_0 \approx 0.031$ , and where  $\bar{\xi}_0$  is the mean-field value of the correlation-length amplitude (Table III). The range of validity of the mean-field theory is determined by the condition  $\tau \gg N_G$ . It has been shown by Anisimov *et al.* [25] that the single-parameter crossover model, based on renormalization-group matching, gives a crossover behavior of the free energy similar to those based on the  $\epsilon$  expansion [26] and on the field theory [55] when cutoff effects are neglected. In the single-parameter model, if the rescaled coupling constant  $u_0/\Lambda c_\rho^4$ , is less than  $u^*$  (the universal renormalization-group-theory fixed-point value of the coupling constant), i.e.,  $\bar{u} = u_0/\Lambda c_\rho^4 u^* < 1$ , the mean-field behavior is recovered in the limit  $\bar{u}\Lambda/\kappa \ll 1$  and controlled by the Gaussian fixed point at which  $\bar{u}\Lambda = 0$ . In simple fluids the cutoff parameter  $\Lambda$  is of order unity (the characteristic microscopic scale  $\xi_D$  is of the order of a molecular size  $v_0^{1/3}$ ). This is why in systems with short-range interactions the crossover to the classical regime is not completed within the critical domain where  $\xi$  is always large. If  $\bar{u} \geq 1$ , the crossover scale is not defined by the single-parameter crossover model. For  $\bar{u} = 1$  all correction-to-scaling terms in the Wegner expansion disappear, and the effective critical exponents within the entire critical domain are equal to their asymptotic (Ising) values. For  $\bar{u} > 1$  the effective critical exponent of the susceptibility for the single-parameter model monotonically increases with increase of  $\tau$  (negative Wegner corrections), and the crossover to the mean-field critical regime never occurs either.

A rigorous analysis of the spherical model led Nicoll and Bhattacharjee [64] to replace the product  $\bar{u}\Lambda/\kappa$  in Eq. (11) for the crossover function  $Y$  by  $\bar{u}(1 + \Lambda^2/\kappa^2)^{1/2}$ , leading to Eq. (3). In this improved crossover model the two crossover parameters  $\bar{u}$  and  $\Lambda$  are separated, i.e., they control the crossover behavior independently, and the mean-field regime is recovered in the limit  $\Lambda/\kappa \ll 1$ . Physically this means that  $\kappa$

is not proportional to the actual correlation length  $\xi$ , but only to that part of the correlation length associated with the critical fluctuations, which should vanish far away from the critical point.

For the case  $\bar{u} < 1$ , which is realized in simple fluids [25], the modification of the crossover function does not have much significance: the crossover is still monotonic and is, in practice, not completed within the critical domain, since  $\xi$  is large and  $\Lambda$  is of order unity. In complex fluids, however, the crossover parameter  $\Lambda$  is not necessarily associated with the actual microscopic cutoff, but may be related to another characteristic spacing on a scale larger than a molecular size. If  $\Lambda$  is small enough (i.e., the characteristic spacing  $\xi_D$  is large), the nonasymptotic behavior of the crossover model as specified by Eqs. (3), (7), and (9) implies that the crossover to the mean field is quite possible within the critical domain, even for  $\bar{u} \geq 1$  [19]. In this case the crossover is not monotonic, since it is controlled by two independent crossover parameters:  $\bar{u} > 1$  is responsible for a negative first Wegner correction amplitude and drives the effective susceptibility exponent upward with increase of  $\tau$ , and small  $\Lambda$  provides a decrease of the exponent downward to the mean-field value  $\gamma = 1$  with further increase of  $\tau$ .

To elucidate the effect of an additional scale on the physical properties of fluids in the critical region, we need more systematic information on the crossover behavior of the susceptibility in different classes of fluids and fluid mixtures, as well as new experiments especially designed to investigate details of the crossover behavior. We realize that our crossover model when extended to complex fluids is essentially phenomenological. The apparently small ‘‘cutoff’’  $\Lambda$  in complex fluids may also be associated with another order parameter, even belonging to a different universality class [27]. In that case a coupling between two order parameters leading to possible multicritical phenomena should be considered.

#### IV. ANALYSIS OF EXPERIMENTAL DATA

One should note that extraction of the actual crossover behavior from experimental data is a very delicate task. Specifically, the susceptibility of fluids is never measured directly. It can be extracted most accurately from light-scattering or turbidity experiments. The interpretation of such data requires reliable information on the correlation function which itself exhibits crossover behavior. Hence, the fit is essentially nonlinear. Moreover, the crossover behavior may be masked by multiple scattering, gravity effects, and impurities close to the critical point, and by noncritical (background) contributions away from the critical point [69]. That is why, in spite of a large number of experimental studies, there are only a few with an accuracy sufficient to recover the actual nonasymptotic critical behavior. We also note that as the convergence of the Wegner series is in doubt, a fit to expansion (1) is dangerous, and an explicit crossover equation for the susceptibility is needed to determine the values of the correction amplitudes.

The intensity of the light scattered from the critical fluctuations in fluid systems as a function of the wave number  $q$  is related to the appropriate isomorphic susceptibility  $\chi$  by [70,71]

$$I_s = C \frac{\chi}{1 + q^2 \xi^2}, \quad (13)$$

where  $C$  is an adjustable coefficient (in arbitrary units). The wave number  $q$  is related to the scattering angle  $\theta$  ( $90^\circ$  in our experiments) as  $q = 4\pi n/\lambda_0 \sin(\theta/2)$ , where  $\lambda_0 = 632.8$  nm, the vacuum wavelength of the incident light, and  $n$  the refractive index. We calculated the values of the refractive index with the aid of the Lorentz-Lorenz relation taking into account the methylpyridine and water components only (at  $20^\circ\text{C}$   $n \approx 1.27$  for all samples). The wave-number dependence of the scattered light intensity is adequately represented by the Ornstein-Zernike correction  $(1 + q^2 \xi^2)^{-1}$  for the actual  $q\xi$  values in the experiments. Hence, to fit experimental data to Eq. (13) with  $\chi$  and  $\xi$  expressed through Eqs. (7) and (8), one needs four adjustable parameters:  $\Lambda$ ,  $\bar{u}$ ,  $c_t$  (or  $c_\rho$ ), and  $C$ . A background term was found insignificant for all the fits except for the sample with  $X = 0.16$ . Variation of the critical-temperature values within the accuracy of their determination did not change the fitting parameters significantly. As the prefactor  $C$  depends on the absolute intensity of the scattered light, we could not independently extract the value of the critical amplitude  $\Gamma_0$ , and hence, the value of the coefficient  $a_0 = c_t c_\rho^2$ . For simplicity we fixed  $a_0 = 1$  in all fits.

In ternary mixtures one has to deal with an additional effect which complicates the interpretation of experimental data. In ‘‘incompressible’’ binary liquid mixtures the path of a zero ordering field corresponds to the path at fixed critical composition. However, in ternary mixtures the path of the zero field corresponds to a path at constant chemical potential  $\mu = \mu_c$  of the third component. Hence, in Eqs. (7) and (8) the variable  $\tau$  means the ‘‘theoretical’’ path at a constant chemical potential. However, the light-scattering measurements are performed at constant concentration. As a consequence, a so-called Fisher renormalization of the critical exponents [72] occurs along the experimental path ( $X = X_c$ ). Specifically, the asymptotic value of the susceptibility exponent  $\gamma = 1.24$  changes to  $\gamma/(1 - \alpha) = 1.39$ . Therefore, one needs to express the theoretical variable  $\tau$  in Eqs. (7) and (8) through the experimentally measured distance to the critical temperature. The relation between the experimental temperature scale  $\tau(X) = |T - T_c(X)|/T$  and the theoretical temperature scale  $\tau(\mu) = |T - T_c(\mu)|/T$  is not analytic [73,74]:

$$\frac{\tau(X)}{\tau_2} \simeq \left( \frac{\tau(\mu)}{\tau_2} \right)^{1-\alpha} \left[ 1 + \left( \frac{\tau(\mu)}{\tau_2} \right)^\alpha \right], \quad (14)$$

where the characteristic temperature  $\tau_2$  is defined by

$$\tau_2 = \left[ A_0 \bar{X} (1 - \bar{X}) \left( \frac{1}{T_c} \frac{dT_c}{d\bar{X}} \right)^2 \right]^{1/\alpha}, \quad (15)$$

and where  $\bar{X}$  indicates the overall mole fraction of NaBr. At  $[\tau(\mu)/\tau_2]^\alpha \gg 1$ ,  $\tau(\mu) \simeq \tau(X)$  and the renormalization of the

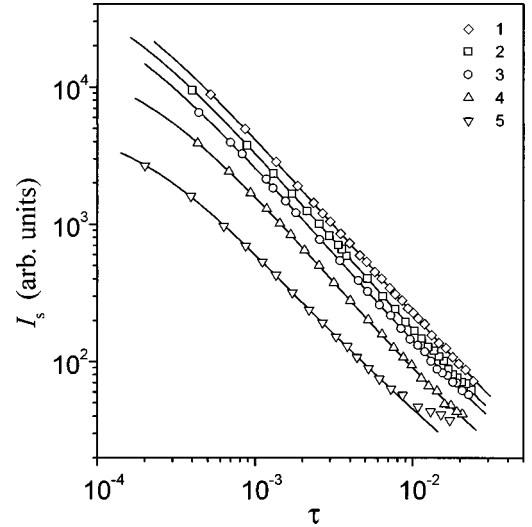


FIG. 2. Scattered intensity  $I_s$  in arbitrary units of 3-methylpyridine+water+sodium bromide solutions as a function of the reduced temperature  $\tau = |T - T_c|/T$ . The symbols indicate the experimental data for the five samples specified in Table I. The curves represent the values calculated with our crossover model.

critical exponents is absent. At  $[\tau(\mu)/\tau_2]^\alpha \ll 1$ ,  $\tau(\mu) \simeq [\tau(X)/\tau_2]^{1/(1-\alpha)}$ , and the exponents are renormalized. The asymptotic critical amplitude  $A_0$  of the weak susceptibility [33] can be expressed through the asymptotic amplitude of the correlation length  $\xi_0$  by the two-scale-factor-universality relation  $A_0 \simeq 0.18 v_0 / \xi_0^3$  [69]. The values of  $dT_c/d\bar{X}$ , deduced from the experimental data, are presented in Table I. The values of  $v_0$  were estimated from the molar density ( $v_0^{1/3} \simeq 3.5$  Å for all the samples). Strictly speaking, the effect of the Fisher renormalization itself should be accounted for the crossover to the mean-field regime. This can be done by using an effective value of  $\alpha$ , which crosses over from  $\alpha = 0.11$  to  $\alpha = 0$ , in Eq. (14). However, this effect is not important for the present analysis, since, in the samples where the crossover is most pronounced, the effect of the Fisher renormalization becomes negligibly small.

In Fig. 2 we plot the scattered-light intensity for the five samples of 3-methylpyridine+water+sodium bromide specified in Table I as a function of the reduced temperature  $\tau = |T - T_c|/T$  at constant composition. The curves represent values calculated with our crossover model. The values obtained for the adjustable parameters  $\Lambda$ ,  $\bar{u}$ ,  $c_t$ , and  $C$  are presented in Table IV together with the standard deviations of the fits. In Table IV, we also give the resulting values for some relevant physical quantities, namely the amplitude  $\xi_0$  of the asymptotic power law  $\xi_0 \tau^{-\nu}$  for the correlation length, the mean-field amplitude  $\bar{\xi}_0$  of the correlation length far away from the critical point, the characteristic length  $\xi_D$  associated with the cutoff  $\Lambda$ , the coefficient  $\Gamma_1$  of the first correction-to-scaling term in Eq. (1), and the characteristic temperature  $\tau_2$  associated with the critical-exponent renormalization [see Eq. (15)]. We note that the amplitude  $\Gamma_1$  is negative for all samples, indicating that the crossover from Ising-like to mean-field behavior is nonmonotonic [19]. This nonmonotonic behavior is shown in Fig. 3, where we plot the effective susceptibility exponent  $\gamma_{\text{eff}} = -\tau d \ln \chi / d\tau$ , with  $\chi$



TABLE IV. Parameters of the crossover model.

Sample	$X$	Adjustable parameters				Standard deviation (%)	Calculated parameters				
		$\Lambda$	$\bar{u}$	$c_t$	$C$		$\xi_0$ (Å)	$\bar{\xi}_0$ (Å)	$\xi_D$ (Å)	$\Gamma_1$	$\tau_2^\alpha$
1	0.0800	0.374	1.57	3.07	1.22	1.6	1.48	1.97	9.21	-1.1	0.13
2	0.1190	0.236	2.29	2.66	1.09	1.8	1.59	2.12	14.7	-2.4	0.091
3	0.1396	0.187	2.02	2.07	1.02	2.4	1.70	2.41	18.6	-2.4	0.061
4	0.1500	0.111	2.68	1.05	0.719	2.4	2.46	3.38	31.0	-3.6	0.017
5	0.1600	0.0460	2.07	0.567	0.427	2.4	2.69	4.60	75.3	-5.4	0.011

represented by the fit of Eq. (7) to the experimental data, as a function of the reduced temperature  $\tau$ .

In Figs. 4 and 5, we show the deviations of the susceptibility values, extracted from the light-scattering data through Eq. (13), from Ising asymptotic behavior. The solid curves in these figures represent the actual crossover behavior implied by our model, and the dotted curves represent asymptotic mean-field behavior. It should be noted that in the mean-field theory the susceptibility diverges at a temperature below the actual critical temperature. From Figs. 3–5 it is evident that the crossover from Ising-like to mean-field behavior becomes more pronounced with an increase of the NaBr concentration, and for the fifth sample with  $X=0.16$  the crossover is practically completed within the critical domain. As can be seen from Figs. 4 and 5, our crossover model describes all the experimental data well. Neither simple Ising behavior nor simple mean-field behavior describes the experimental data. Instead a crossover between the Ising regime and the mean-field regime dominates in the temperature range  $10^{-4} < \tau < 10^{-2}$ . The tendency to approach mean-field behavior away from the critical temperature becomes more and more pronounced with an increase of the salt concentration, and for  $X=0.16$  mean-field behavior prevails within  $10^{-3} < \tau < 10^{-2}$  (Fig. 5). The experimental suscepti-

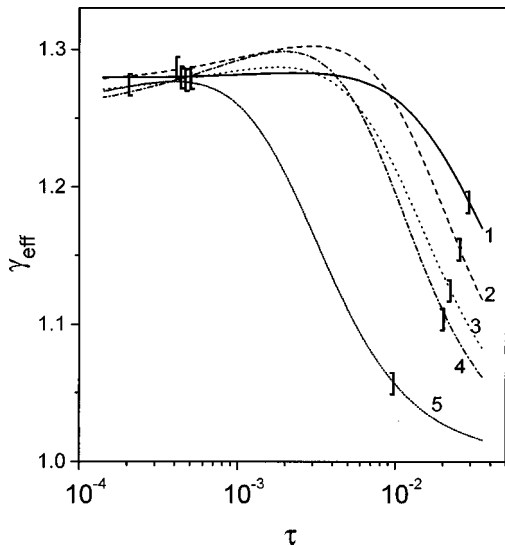


FIG. 3. Effective susceptibility exponent  $\gamma_{\text{eff}} = -\tau d \ln \chi / d\tau$  for the five samples of the 3-methylpyridine+water+sodium bromide system calculated from our crossover model as a function of  $\tau$ . The brackets [ ] mark the temperature intervals of the actual fit to experimental data for each sample.

bility data at the largest concentration  $X=0.16$  in the temperature range  $\tau > 10^{-2}$  systematically deviate from the calculated values. We speculate that this effect may arise from an anomaly in the light scattering related to another possible phase transition at low temperatures and higher salt concentrations. Therefore, we fitted the model to the experimental data for this sample only within the range  $\tau < 10^{-2}$ . As mentioned earlier, for all the samples the crossover is characterized by a negative value of the first Wegner correction amplitude  $\Gamma_1$ . Hence the crossover is sharp and is not monotonic:  $\gamma_{\text{eff}}$  as a function of  $\tau$  goes through a maximum. Another specific feature of the crossover behavior of  $\gamma_{\text{eff}}$  is related to the fact that the investigated solution is a ternary system. As a consequence, the susceptibility exponent changes its asymptotic value from  $\gamma$  to  $\gamma/(1-\alpha)$  due to Fisher renormalization. The effect of the renormalization depends on the parameter  $\tau_2$  (listed in Table IV), and the effect is less noticeable for larger concentrations of NaBr. Figure 6

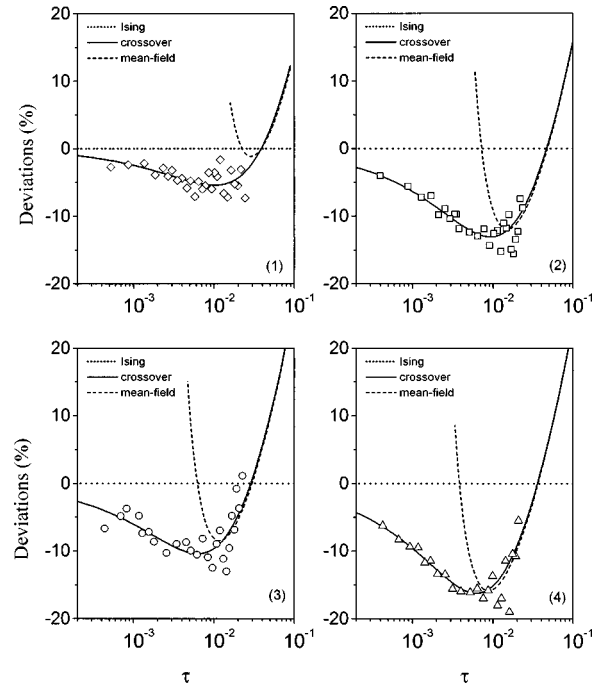


FIG. 4. Deviations of the observed susceptibility of 3-methylpyridine+water+sodium bromide solutions from Ising asymptotic behavior (dashed line) for four samples (1)  $X=0.08$ , (2)  $X \approx 0.12$ , (3)  $X \approx 0.14$ , and (4)  $X=0.15$ . The dotted curves represent mean-field asymptotic behavior, and the solid curves the actual crossover behavior. Note that the mean-field susceptibility diverges at a temperature below the actual critical temperature.

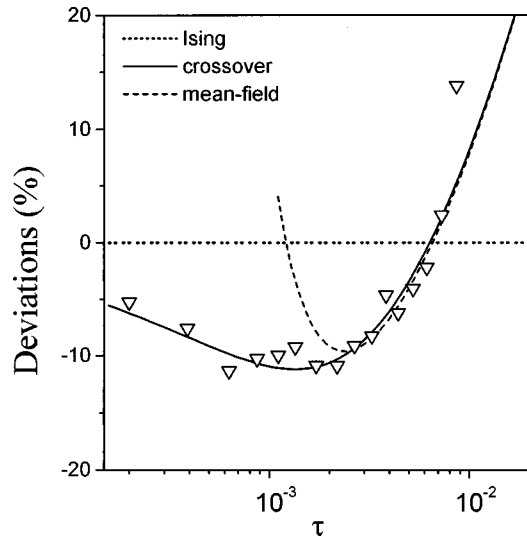


FIG. 5. Deviations of the observed susceptibility from the Ising asymptotic behavior (dashed line) for the sample with  $X=0.16$ . The dotted curve represents the mean-field asymptotic behavior, and the solid curve the actual crossover behavior.

demonstrates the Fisher renormalization for the sample  $X=0.08$  in which the effect is most pronounced. While the solid curve represents the effective susceptibility exponents along the experimental path  $X=\text{const}$  [ $\gamma_{\text{eff}} = -\tau d \ln \chi / d\tau(X)$ ], the dashed curve represents the values along the theoretical path  $\mu=\text{const}$  [ $\gamma_{\text{eff}} = -\tau d \ln \chi / d\tau(\mu)$ ] in accordance with Eq. (14). The renormalization becomes less important with increase of salt concentration as  $dT_c/dX$  and  $A_0$  decrease in spite of increasing  $X$ . For the sample  $X=0.16$ , the effect of the renormalization is negligible.

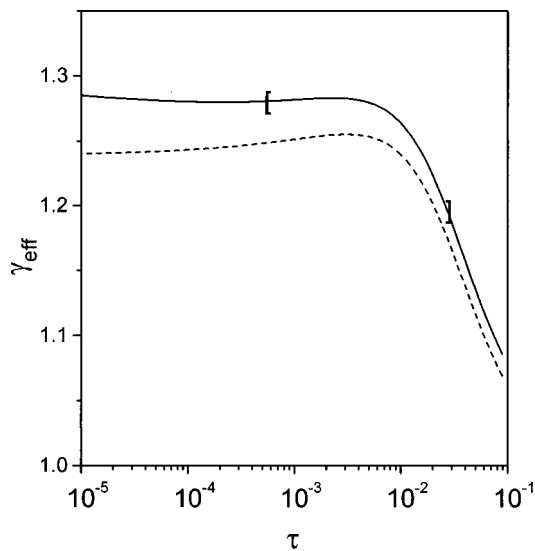


FIG. 6. Effective susceptibility exponent  $\gamma_{\text{eff}}$  for the sample with  $X=0.08$  as a function of  $\tau$ . The solid curve represents  $\gamma_{\text{eff}}$  along the experimental path  $X=\text{const}$  and the dotted curve represents  $\gamma_{\text{eff}}$  along the theoretical path  $\mu=\text{const}$ . Along the theoretical path,  $\gamma_{\text{eff}}$  asymptotically approaches the Ising value  $\gamma=1.24$ . Along the experimental path,  $\gamma_{\text{eff}}$  asymptotically approaches the renormalized value  $\gamma/(1-\alpha)=1.39$ . The brackets [ ] mark the temperature range of the actual fit to experimental data for this sample.

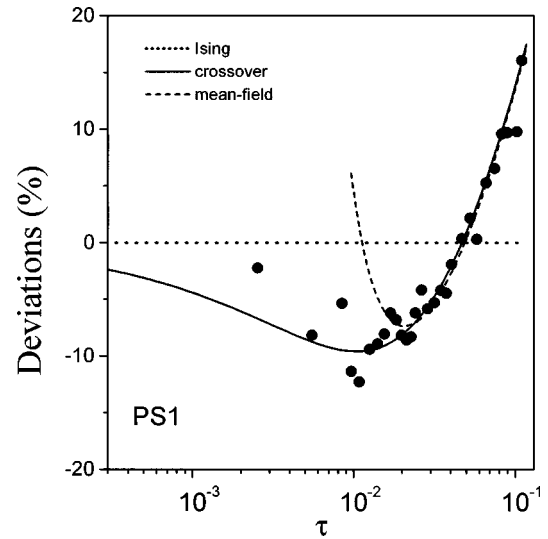


FIG. 7. Deviations of the susceptibility, extracted from experimental neutron-scattering data [27], from Ising asymptotic behavior (dashed line) for a polystyrene-deuterocyclohexane solution ( $M_w=28.000$ ). The dotted curve represents the mean-field asymptotic behavior, and the solid curve the actual crossover behavior.

## V. DISCUSSION

The crossover behavior of the susceptibility of MP+water+sodium bromide solutions shows a striking similarity with the crossover behavior previously observed for the susceptibility in nonaqueous ionic solutions with low dielectric constant [19] and in polymer solutions [27] as illustrated in Figs. 7 and 8. In all these cases the crossover of the susceptibility is sharp and nonmonotonic and an additional characteristic length scale is revealed. The mean-field behavior becomes

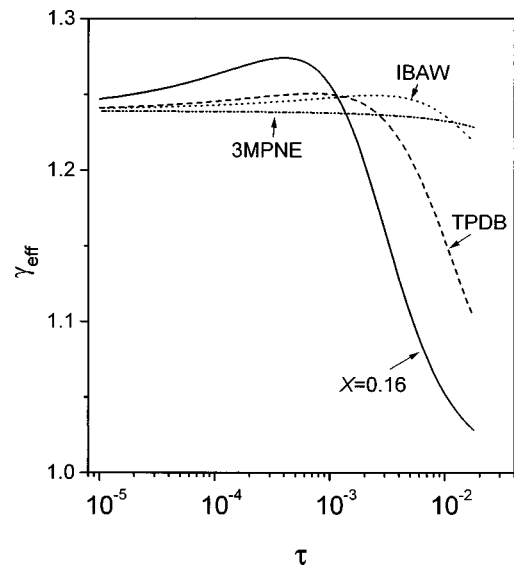


FIG. 8. Effective susceptibility exponent  $\gamma_{\text{eff}} = -\tau d \ln \chi / d\tau$  as a function of  $\tau$  for a mixture of isobutyric acid and water (IBAW), a nonaqueous ionic solution of tetra-*n*-butyl ammonium picrate in 1,4-butanediol/1-dodecanol (TPDB), a mixture of 3-methylpentane and nitroethane (3MPNE) [19], and for the  $X=0.16$  sample of the ternary mixture 3-methylpyridine+water+sodium bromide (this work).

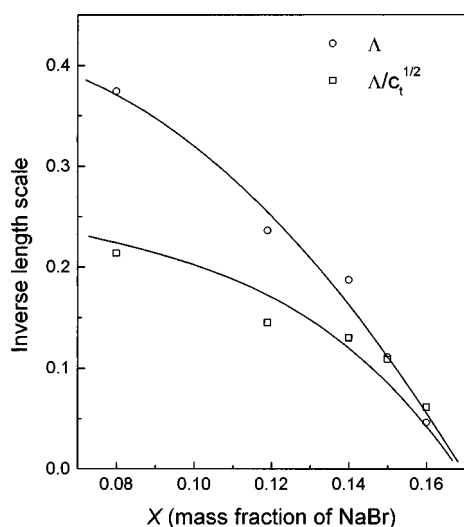


FIG. 9. Inverse dimensionless (reduced by the intermolecular distance) characteristic length scale  $\Lambda$  and the ratio  $\Lambda/c_t^{1/2}$  as a function of the salt concentration. The symbols indicate the values deduced from the fits of the crossover model to experimental data. The solid curves are given as a guidance.

more pronounced when this additional length increases. In polymer solutions this additional length has a clear physical meaning: it is of the order of the size of the polymer molecules: the cutoff parameter  $\Lambda \propto \xi_D^{-1}$  is of the order of the inverse radius of gyration which diverges when the molecular weight  $M_w$  becomes infinite [27]. The limit  $M_w \rightarrow \infty$  corresponds to the tricritical  $\theta$  point [28] in which  $\Lambda \propto c_t \rightarrow 0$  as  $M_w^{-1/2}$ , while  $\Lambda/c_t^{1/2} \rightarrow 0$  as  $M_w^{-1/4}$ .

The origin of the additional characteristic length scale in the system MP+H<sub>2</sub>O+NaBr is not clearly understood. The additional length scale could stem from a possible association of 3-methylpyridine molecules. With an increasing concentration of NaBr, the size of the clusters may increase since the solubility of NaBr in water is much higher compared to its solubility in 3-methylpyridine. A recurring theme in the earlier light-scattering studies of closely related systems MP+water+sodium chloride [30], MP+water+heavy water+potassium iodide [31], and ethanol+water+potassium carbonate [32] is a progressive trend to mean-field behavior with increase of the electrolyte concentration. This trend has been attributed [31,32,75,76] to an electrolyte-induced structuring in these systems. Small angle x-ray and neutron-scattering measurements in these systems are desirable to verify the existence of this additional length scale as well as its dependence upon the electrolyte concentration.

An analogy between dilute polymer solutions and solutions of electrolytes was discussed by Fisher [11]. It is also interesting that the phase diagram of a hydrosoluble polymer [77] is similar to that presented in Fig. 1, with the number of monomer units playing the same role as the salt concentration. The possibility of a multicritical Lifshitz point in which two fluid phases in an electrolyte solution coexist with a microheterogeneous charge-density wave phase was suggested in Ref. [78]. Hence, in ionic solutions the additional characteristic length may be associated with some kind of a supramolecular structure, such as the one predicted in Ref.

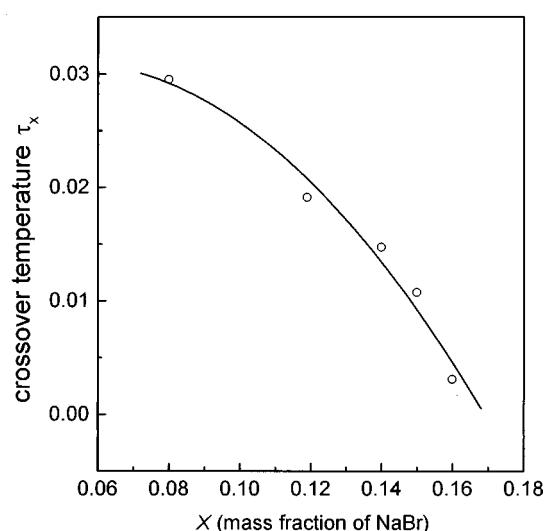


FIG. 10. Crossover temperature  $\tau_x$  as a function of the salt concentration.  $\tau_x$  is defined as the value of  $\tau$  which corresponds to the inflection point in the dependence of  $\gamma_{\text{eff}}$  on  $\tau$  in Fig. 3.

[78]. Figure 9 shows the evolution of the cutoff parameter  $\Lambda$  and the ratio  $\Lambda/c_t^{1/2} = \bar{\xi}_0/\xi_D$  with an increase of the salt concentration. While the parameter  $\bar{u}$  does not significantly change, both  $\Lambda$  and  $c_t$ , as well as the ratio  $\Lambda/c_t^{1/2}$ , decrease with increase of the salt concentration. The solid curves are given as a guide to show the tendency of these parameters to decrease or even vanish at a certain concentration of NaBr  $X = X_0 \approx 0.17$ . This conclusion is strongly supported by the behavior of the crossover temperature scale  $\tau_x \propto \Lambda^2/c_t$  defined as the coordinate of the inflection point in the dependence of  $\gamma_{\text{eff}}$  on  $\tau$  shown in Fig. 10 as a function of the salt concentration. We note also that  $X \approx 0.17$  corresponds to an inflection point of the critical temperature line (Fig. 1). If the observed tendency of increasing characteristic length  $\xi_D \propto \Lambda^{-1}$  results in a divergence of  $\xi_D$  at  $X = X_0$ , this concentration would, indeed, correspond to a multicritical point of some kind. Further studies need to be performed to answer this intriguing possibility.

#### ACKNOWLEDGMENTS

We thank T. Narayanan for inspiring us to take up this problem and for many rewarding discussions. We have also benefited from stimulating discussions with M. E. Fisher, J. M. H. Levelt Sengers, and the late K. S. Pitzer. We have appreciated encouragement received from E. S. R. Gopal and cooperation from B. M. Jaffar Ali. The research at the Indian Institute of Science was supported by the Department of Science and Technology and the Department of Atomic Energy, Government of India. The research of A. A. P. was supported by the American Chemical Society under PRF Grant No. 30693-AC9. The research of M. A. A. and J. V. S. was supported by the Division of Chemical Sciences of the Office of Basic Energy Sciences of the U.S. Department of Energy under Grant No. DE-FG02-95ER-14509.

- [1] V. Degiorgio, R. Piazza, M. Corti, and C. Minero, *J. Chem. Phys.* **82**, 1025 (1985).
- [2] M. Corti and V. Degiorgio, *Phys. Rev. Lett.* **55**, 2005 (1985).
- [3] G. Dietler and D. S. Cannell, *Phys. Rev. Lett.* **60**, 1852 (1988).
- [4] K. Hamano, N. Kuwahara, I. Mitsushima, K. Kubota, and T. Kamura, *J. Chem. Phys.* **94**, 2172 (1991).
- [5] H. G. Glasbrenner and H. Weingärtner, *J. Phys. Chem.* **93**, 3378 (1989).
- [6] H. Weingärtner, S. Wiegand, and W. Schröer, *J. Chem. Phys.* **96**, 848 (1992).
- [7] H. Weingärtner, T. Merkel, S. Käshammer, W. Schröer, and S. Wiegand, *Ber. Bunsenges. Phys. Chem.* **97**, 970 (1993).
- [8] W. Schröer, S. Wiegand, and H. Weingärtner, *Ber. Bunsenges. Phys. Chem.* **97**, 975 (1993).
- [9] K. J. Zhang, M. E. Briggs, R. W. Gammon, and J. M. H. Levelt Sengers, *J. Chem. Phys.* **97**, 8692 (1992).
- [10] S. Wiegand, J. M. H. Levelt Sengers, K. J. Zhang, M. E. Briggs, and R. W. Gammon, *J. Chem. Phys.* **106**, 2777 (1997).
- [11] M. E. Fisher, *J. Stat. Phys.* **75**, 1 (1994).
- [12] J. M. H. Levelt Sengers and J. A. Given, *Mol. Phys.* **80**, 899 (1993).
- [13] K. S. Pitzer, *Acc. Chem. Res.* **22**, 333 (1990).
- [14] H. Weingärtner, M. Kleemeier, S. Wiegand, and W. Schröer, *J. Stat. Phys.* **78**, 169 (1995).
- [15] J. M. H. Levelt Sengers, A. H. Harvey, and S. Wiegand, in *Equations of State for Fluids and Fluid Mixtures*, edited by J. V. Sengers, M. B. Ewing, R. F. Kayser, C. J. Peters, and H. J. White, Jr. (Blackwell Scientific, Oxford, in press).
- [16] T. Narayanan and K. S. Pitzer, *Phys. Rev. Lett.* **73**, 3002 (1994).
- [17] T. Narayanan and K. S. Pitzer, *J. Phys. Chem.* **98**, 9170 (1994).
- [18] T. Narayanan and K. S. Pitzer, *J. Chem. Phys.* **102**, 8118 (1995).
- [19] M. A. Anisimov, A. A. Povodyrev, V. D. Kulikov, and J. V. Sengers, *Phys. Rev. Lett.* **75**, 3146 (1995); **76**, 4095 (1996).
- [20] P. Chieux, J.-F. Jal, L. Hily, J. Dupuy, F. Leclercq, and P. Damay, *J. Phys. (Paris) Colloq.* **52**, C5-3 (1991); P. Chieux, *ibid.* **52**, C5-373 (1991).
- [21] G. Meier, B. Momper, and E. W. Fischer, *J. Chem. Phys.* **97**, 5884 (1992); G. Meier, D. Schwahn, K. Mortensen, and S. Janssen, *Europhys. Lett.* **22**, 577 (1993).
- [22] D. Schwahn, K. Mortensen, and H. Y. Madeira, *Phys. Rev. Lett.* **58**, 1544 (1987); S. Janssen, D. Schwahn, and T. Springer, *Phys. Rev. Lett.* **68**, 3180 (1992).
- [23] E. K. Hobbie, L. Read, C. C. Huang, and C. C. Han, *Phys. Rev. E* **48**, 1579 (1993).
- [24] H. Seto, D. Schwahn, M. Nagao, E. Yokoi, S. Komura, M. Imai, and K. Mortensen, *Phys. Rev. E* **54**, 629 (1996).
- [25] M. A. Anisimov, S. B. Kiselev, J. V. Sengers, and S. Tang, *Physica A* **188**, 487 (1992).
- [26] M. Y. Belyakov and S. B. Kiselev, *Physica A* **190**, 74 (1992).
- [27] Y. B. Melnichenko, M. A. Anisimov, A. A. Povodyrev, G. D. Wignall, J. V. Sengers, and W. A. Van Hook, *Phys. Rev. Lett.* **79**, 5266 (1997).
- [28] P. G. de Gennes, *Scaling Concepts in Polymer Physics* (Cornell University Press, Ithaca, NY, 1979).
- [29] S. Venkatachalam, A. Kumar, and E. S. R. Gopal, *J. Chem. Phys.* **103**, 6645 (1995).
- [30] T. Narayanan and A. Kumar, *Phys. Rep.* **249**, 135 (1994).
- [31] T. Narayanan, A. Kumar, S. Venkatachalam, J. Jacob, and B. V. Prafulla, *J. Chem. Phys.* **102**, 9653 (1995).
- [32] B. M. Jaffar Ali and A. Kumar, *J. Chem. Phys.* **107**, 8020 (1997).
- [33] M. A. Anisimov, E. E. Gorodetskii, V. D. Kulikov, and J. V. Sengers, *Phys. Rev. E* **51**, 1199 (1995).
- [34] Z. Y. Chen, P. C. Albright, and J. V. Sengers, *Phys. Rev. A* **41**, 3161 (1990).
- [35] Z. Y. Chen, A. Abbaci, S. Tang, and J. V. Sengers, *Phys. Rev. A* **42**, 4470 (1990).
- [36] B. V. Prafulla, Ph.D. thesis, Indian Institute of Science, Bangalore, 1993.
- [37] J. R. Leigh, *Temperature Measurement and Control* (Pergamon, London, 1988).
- [38] A. J. Bray and R. F. Chang, *Phys. Rev. A* **12**, 2594 (1975).
- [39] J. V. Sengers, in *Supercritical Fluids: Fundamentals for Application*, edited by E. Kiran and J. M. H. Levelt Sengers (Kluwer, Dordrecht, 1994), p. 231.
- [40] I. Prigogine and R. Defay, *Chemical Thermodynamics* (Logmans, London, 1954).
- [41] M. A. Anisimov, V. A. Agayan, A. A. Povodyrev, J. V. Sengers, and E. E. Gorodetskii, *Phys. Rev. E* **57**, 1946 (1998).
- [42] J. V. Sengers and J. M. H. Levelt Sengers, *Annu. Rev. Phys. Chem.* **37**, 189 (1986).
- [43] A. J. Liu and M. E. Fisher, *Physica A* **156**, 35 (1989).
- [44] S.-Y. Zinn and M. E. Fisher, *Physica A* **226**, 168 (1996).
- [45] F. J. Wegner, *Phys. Rev. B* **5**, 4529 (1972).
- [46] N. D. Mermin and J. J. Rehr, *Phys. Rev. Lett.* **26**, 1155 (1971).
- [47] J. F. Nicoll, *Phys. Rev. A* **24**, 2203 (1981).
- [48] F. C. Zhang and R. K. P. Zia, *J. Phys. A* **15**, 3303 (1982).
- [49] M. Ley-Koo and M. S. Green, *Phys. Rev. A* **23**, 2650 (1981).
- [50] J. S. Kouvel and M. E. Fisher, *Phys. Rev.* **136**, A1626 (1964).
- [51] P. Seglar and M. E. Fisher, *J. Phys. C* **13**, 66 (1980).
- [52] M. E. Fisher, *Phys. Rev. Lett.* **57**, 1911 (1986).
- [53] D. R. Nelson, *Phys. Rev. B* **11**, 3504 (1975).
- [54] I. D. Lawrie, *J. Phys. A* **9**, 961 (1976).
- [55] C. Bagnuls and C. Bervillier, *Phys. Rev. B* **32**, 7209 (1985).
- [56] E. Luijten, H. W. J. Blöte, and K. Binder, *Phys. Rev. E* **56**, 6540 (1997).
- [57] A. J. Liu and M. E. Fisher, *J. Stat. Phys.* **58**, 431 (1990).
- [58] V. Dohm, *Phys. Scr.* **49**, 46 (1993).
- [59] C. Bagnuls and C. Bervillier, *Phys. Lett. A* **195**, 163 (1994).
- [60] G. Zalczer and D. Beysens, *J. Chem. Phys.* **92**, 6747 (1990).
- [61] J. D. Shanks, Ph.D. thesis, University of Maryland, College Park, MD, 1986 (unpublished).
- [62] H. Güttinger and D. S. Cannell, *Phys. Rev. A* **24**, 3188 (1981).
- [63] R. F. Chang, H. Burstyn, and J. V. Sengers, *Phys. Rev. A* **19**, 866 (1979).
- [64] J. F. Nicoll and J. K. Bhattacharjee, *Phys. Rev. B* **23**, 389 (1981).
- [65] J. F. Nicoll and P. C. Albright, *Phys. Rev. B* **31**, 4576 (1985).
- [66] J. C. Le Guillou and J. Zinn-Justin, *J. Phys. (Paris)* **48**, 19 (1987).
- [67] M. A. Anisimov and J. V. Sengers, in *Equations of State for Fluids and Fluid Mixtures* (Ref. [15]).
- [68] S. Tang, J. V. Sengers, and Z. Y. Chen, *Physica A* **179**, 344 (1991).
- [69] M. A. Anisimov, *Critical Phenomena in Liquids and Liquid Crystals* (Gordon and Breach, Philadelphia, 1991).
- [70] M. E. Fisher, *J. Math. Phys.* **5**, 944 (1964).
- [71] J. V. Sengers and J. M. H. Levelt Sengers, in *Progress in Liquid Physics*, edited by C. A. Croxton (Wiley, New York, 1978), p. 103.

- [72] M. E. Fisher, *Phys. Rev.* **176**, 237 (1968).
- [73] M. A. Anisimov and S. B. Kiselev, *Thermal Physics Reviews*, edited by A. E. Scheindlin and V. E. Fortov, Soviet Technology Reviews, Section B, Vol. 3, Part 2 (Harwood Academic, 1992), p. 1.
- [74] H. Y. Cheng, M. A. Anisimov, and J. V. Sengers, *Fluid Phase Equilibria* **128**, 67 (1997).
- [75] B. V. Prafulla, T. Narayanan, and A. Kumar, *Phys. Rev. A* **46**, 7456 (1992).
- [76] B. M. Jaffar Ali and A. Kumar, *Phys. Lett. A* **237**, 257 (1998).
- [77] S. Bekiranov, R. Bruinsma, and P. Pincus, *Phys. Rev. E* **55**, 577 (1997).
- [78] V. M. Nabutovskii, N. A. Nemov, and Yu. G. Peisakhovich, *Zh. Éksp. Teor. Fiz.* **79**, 2196 (1980) [*Sov. Phys. JETP* **52**, 1111 (1980)]; *Phys. Lett. A* **79**, 98 (1980); *Mol. Phys.* **54**, 979 (1985).